International Journal of Microwave and Wireless Technologies

cambridge.org/mrf

Drop deformation estimate with multi-polarization radar

Yuliya Averyanova, Anna Rudiakova and Felix Yanovsky

National Aviation University, Prospect Lubomyra Guzara, 1, Kyiv 03058, Ukraine

Research Paper

Cite this article: Averyanova Y, Rudiakova A, Yanovsky F (2020). Drop deformation estimate with multi-polarization radar. *International Journal of Microwave and Wireless Technologies* **12**, 870–877. https://doi.org/10.1017/S1759078720000732

Received: 30 November 2019
Revised: 6 May 2020
Accepted: 9 May 2020
First published online: 10 June 2020

Key words:
Radar; System Applications and Standards

Author for correspondence:
Yuliya Averyanova, E-mail: ayua@nau.edu.ua

Abstract

This paper considers the ability of polarization measurements for microwave remote sensing of clouds and precipitation. The simulation of reflections from liquid hydrometeors with a multi-polarization radar system is presented. The mathematical expression of energy received by a radar antenna with arbitrary polarization is obtained. The simulation of the energy redistribution of the signal reflected from liquid hydrometeors assembled over the antennas of multi-polarimetric radar for different wind conditions and different drop-size distributions is obtained and analyzed. The simulation results demonstrate the possibility to register wind and wind-related phenomena by polarimetric radar. The results of the paper can also be used to exclude an impact of drop vibration or oscillation into the radar signal to eliminate errors and underestimation during parameter measurements. The approach to segregate the reflected signal magnitude variations due to the wind-related phenomena from other factors is discussed.

Introduction

Radars have become a powerful tool for solving a range of meteorological tasks during the last few decades. Meteorological radars have shown their good potential in watching atmospheric formation and detection of weather hazards [1–3].

During these decades, meteorological radars have evolved from the ordinary noncoherent radars to the modern combined Doppler and polarimetric radar systems during their development.

First, weather surveillance radars measured only radar reflectivity and were used mostly to detect dangerous thunderstorms or convective clouds and help to avoid them. Then, further progress and development of Doppler radars allowed measurement of the radial velocities of radar signal reflectors. The development of meteorological radars continued and resulted in radar systems that take into account the polarization characteristics of electromagnetic waves as well. These systems are known as polarimetric meteorological radars. The operation of the modern polarimetric radars is based on transmitting the vertically or horizontally polarized sounding waveforms and receiving the reflected copolarized or cross-polarized components of the backscattered electromagnetic waves. Modern polarimetric radar systems use mostly two receivers that allow simultaneous measurement of copolarized and cross-polarized components of the backscattered electromagnetic wave. Then polarimetric radar variables can be calculated. Modern polarimetric radars are sensitive to the shape of the hydrometeors and allow obtaining information about the microstructure of the atmospheric object under the study.

Investigation of hydrometeors, as well as their behavior under different atmospheric conditions, is a task of great interest for radar meteorology. Drops deformation and vibration are essential for rainfall measurements and precipitation intensity estimation with dual-polarized radars. The well-known raindrops study is probably started in the 19th century by Rayleigh [4]. The investigations continued in the 20th century and have shown that drop shape deformation and vibration can be noticed in drops with diameters more than 1 mm. Then, many models were developed to connect the drop shape and the drop axis ratio under different atmospheric conditions [5–11]. The drop axis ratio is a required parameter in radar meteorology, and it is usually defined as the ratio of the largest vertical (c) and horizontal axes (a and b) of the raindrop that can be represented as a spheroid. Spheroid and, then, ellipsoid (Fig. 1) are convenient and accepted models of falling drop that is under the action of weight force, drag force, and surface tension. Figure 2 shows the images of falling drops of different sizes and illustrates the dependence of drop oblateness (or variation of the drop axis ratio) on their sizes.

The drop shape is also affected by the character of air that is blowing around it. Moreover, the falling drops are under the effect of internal and external forces. The force interaction results in drop behavior similar to the behavior of the objects with unstable shapes. This leads to the drops vibration or oscillation during their falling. The drop oscillation, in turn,

© Cambridge University Press and the European Microwave Association 2020

CAMBRIDGE UNIVERSITY PRESS

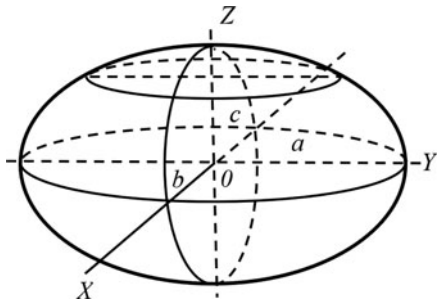


Fig. 1. Approximation of drop with ellipsoid; *a*, *b*, and *c* are the horizontal and vertical axes of a drop ellipsoid.

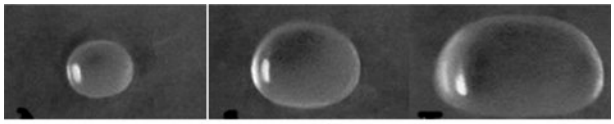


Fig. 2. Steady falling drops: (a) $D = 2.8$ mm, (b) $D = 4.8$ mm, and (c) $D = 6.3$ mm.

makes an impact on radar-based precipitation prediction resulting in errors and underestimation in the axis ratio [12]. At the same time, the drop shape fluctuations can reflect important information about behavior, characteristics, and structure of reflecting objects. The character of vibrations can be provided by the features of the object, their interaction with medium, and even influence of dynamic phenomena such as wind and turbulence onto the unstable shape objects. In [13], the analysis of the drop deformation rate under the effect of atmospheric dynamic phenomena was performed as well as the approach to connect polarization characteristics of reflected radar signals with the deformation. This approach is quite untraditional as nowadays polarization is used for clouds and precipitation microstructure identification mostly. In [14, 15], the possibility of the radar polarimetry to estimate the impact of drop oscillation onto the reflected radar signal to improve information about drop shape parameters was considered. In this paper, we consider the possibility of radar polarimetry to estimate the drop deformation due to wind influence. According to approaches developed in [14, 15], the wind and wind-related phenomena lead to the liquid drop deformation resulting in variation in the drop axis ratio. This factor was taken into account in the developed model.

Mathematical model of energy received with multi-polarization radar

The mathematical model of energy redistribution over the antennas of multi-polarization radar was developed in [16] and then enhanced in [17]. This model considers the case with a single-sounding antenna with a polarization angle δ_i and multiple-receiving antennas with the set of polarization angles $\{\delta_{r_k}\}$. For calculation simplification, the zeroth azimuthal and elevation angles were selected. In the mathematical model, the direction of the y axis is the same as the sounding direction, the z axis is directed to the zenith, and the x axis is perpendicular to both previous. According to [18], we can write the following expressions for the x- and z-components of scattered rain-drop field:

$$E_x = E_x^{sph}\left[1 + 0.4\frac{\varepsilon - 1}{\varepsilon + 2}\rho(t)\right], \quad E_z = E_z^{sph}\left[1 - 0.8\frac{\varepsilon - 1}{\varepsilon + 2}\rho(t)\right]$$

where

$$E_x^{sph} = E^{sph}\sin\delta_i,$$

$$E_z^{sph} = E^{sph}\cos\delta_i,$$

$$E^{sph} = E_0\frac{D^3}{8}\frac{\varepsilon - 1}{\varepsilon + 2}\cos\left[\omega_0 t + 2k_0 r(t)\right],$$

$$\rho(t) = \rho_0 + \Delta\rho\cos\left[\Omega t + \phi\right],$$

D is the equivalent spherical rain-drop of the same volume diameter, ε is the relative dielectric permittivity of water, ω_0 is the sounding angular frequency, k_0 is the sounding wave number, $r(t)$ is the rain-drop radius-vector projection to the sounding direction, ρ is drop axis ratio that corresponds to the ratio between the vertical and horizontal rain-drop sizes, $\rho_0 = 1 - c/a$ corresponds to the mean drop axis ratio, a and c are the horizontal and vertical axes of a drop spheroid (corresponds to the horizontal and vertical axes of a drop ellipsoid respectively shown in Fig. 1), $\Delta\rho$ is the magnitude of drop axis ratio variation, and Ω and ϕ are the angular frequency and the initial phase of rain-drop vibration, respectively.

The scattered field received by k-th antenna can be expressed as:

$$E_k = E_x\sin\delta_{r_k} + E_z\cos\delta_{r_k}.$$

Using the above expressions for the E_x and E_z, we can obtain the following:

$$E_k = E^{sph}\left[\cos\left(\delta_{r_k} - \delta_i\right) - \frac{\rho(t)}{2}\left\{\cos\left(\delta_{r_k} - \delta_i\right) + 3\cos\left(\delta_{r_k} + \delta_i\right)\right\}\right].$$
$$= E^{sph}\left[A_0(\delta_i, \delta_{r_k}) - \rho(t)A_1(\delta_i, \delta_{r_k})\right] \quad (1)$$

The dependencies of $A_1(\delta_i, \delta_{r_k})$ and $A_0(\delta_i, \delta_{r_k})$ on sounding and receiving antennas' polarization angles are shown in Fig. 3. As can be seen from equation (1), in order to find the combination of incident and receiving antennas' polarization angles which give the same response as from the spherical rain-drop of the corresponding volume, one need to solve the system of equations:

$$\begin{cases} A_0(\delta_i, \delta_{r_k}) = 1, \\ A_1(\delta_i, \delta_{r_k}) = 0. \end{cases}$$

There is a single combination of incident and receiving antennas' polarization angles within the [0°, 90°] range, both equal to about 54.7°, that is in agreement with the [18].

This fact is important because the selection of polarization angle allows excluding the impact of polarization features of the object under the study into the reflecting signal or vice versa to increase the polarization sensitivity of the receiving antenna and thus, to strengthen the potential for further analysis of polarization characteristics.

To evaluate the variable component of the scattered field, we need to consider the situation with zeroth $A_0(\delta_i, \delta_{r_k})$ coefficient. Therefore, the polarization angle of the receiving antenna should

https://doi.org/10.1017/S1759078720000732 Published online by Cambridge University Press

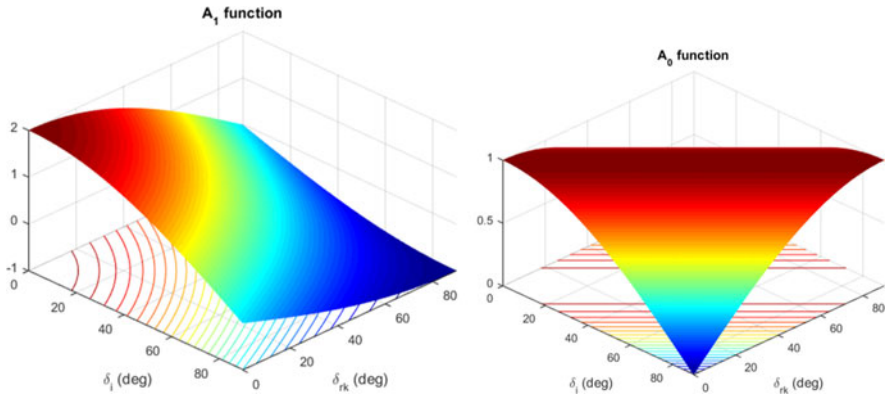


Fig. 3. Dependencies of $A_1(\delta_i, \delta_{r_k})$ and $A_0(\delta_i, \delta_{r_k})$ on sounding and receiving antennas' polarization angles.

be at 90° greater than one of the sounding antennas. In this case, we can write the following expression for the so-called "vibration" scattered field:

$$E_k|_{\delta_{r_k}=\pi/2+\delta_i} = E^{sph}[\rho(t)\{3\sin(\delta_i)\cos(\delta_i)\}] = E^{sph}\rho(t)A_{vib}(\delta_i).$$

In nature, the sounding waveform is reflected from the assemble of the drops. The expression that corresponds to the more realistic situation of multiple drops was developed. The magnitude of the electrical field component at the receiver for drops assemble under single scattering assumption can be represented by the following expression:

$$E_k = \sum_{n=1}^{N} E_n^{sph}[A_0(\delta_i, \delta_{r_k}) - A_1(\delta_i, \delta_{r_k})\{\rho_{0_n} + \Delta\rho_n \cos[\Omega_n t + \phi_n]\}], \quad (2)$$

where the index n corresponds to the n-th drop, and the E_n^{sph} accounts for the raindrop Doppler shift frequency ω_n. Using the phase detection, the following dependence of the output detector signal can be written as:

$$U_k = \sum_{n=1}^{N} |E_n^{sph}|[A_0(\delta_i, \delta_{r_k}) - A_1(\delta_i, \delta_{r_k})\rho_{0_n}]\cos(\omega_n t + \psi_n) + \frac{1}{2}A_1(\delta_i, \delta_{r_k})\sum_{n=1}^{N}|E_n^{sph}|\Delta\rho_n\{\cos[(\omega_n + \Omega_n)t + \psi_n + \phi_n] + \cos[(\omega_n - \Omega_n)t + \psi_n - \phi_n]\} \quad (3)$$

In order to account the drop size distribution, (2) can be represented as follows:

$$E_k = \int_{D_{\min}}^{D_{\max}} E^{sph}(D)[A_0(\delta_i, \delta_{r_k}) - A_1(\delta_i, \delta_{r_k})\{\rho_0(D) + \Delta\rho(D)\cos[\Omega(D)t + \phi(D)]\}]N(D)dD \quad (4)$$

where $N(D)$ corresponds to some of the known drop size distributions.

In the developed model, D ranged from 0.1 to 7.9 mm.

The general case of raindrop size distribution is gamma distribution:

$$N(D) = N_0 D^{\mu}\exp\left(-\frac{3.67+\mu}{D_0}D\right) \quad (5)$$

where D_0 is the equivalent diameter of the median drop, that depends on rain intensity, $N_0 = 8000/\text{mm/m}^3$ (typical value according to [19]), and μ is the parameter of the distribution spread that also indicates the number of drops of particular sizes.

It is indicated in [20] that μ can take values between 0 and 15, but usually are at the beginning of the indicated range.

The dependence of drop vibration fundamental frequency and magnitude on a drop size are given in [10]:

$$\Delta\rho(D) = 3.6\times10^{-3}D_0^2 + 2.13\times10^{-2}D_0,$$

$$\Omega(D) = \left(\frac{8\sigma}{\rho_w(D/2)^3}\right)^{1/2},$$

where σ (N/m) is the surface tension and ρ_w (kg/m^3) the density of water.

Model (4) takes into account the drop vibration as well as the drop deformation extent depending on the external force applied to the drops.

The model relies on the behavior peculiarities of the different liquid hydrometeors that can change their shape and orientation under the influence of the wind and wind-related phenomena. These phenomena are considered as some external influence. The intensity of this influence can be evaluated trough the extent of the change of drops orientation, drops shape variations, and their vibrations. The components of the model of the field scattered by rain-drop (such as rain-drop radius-vector projection, drop axis ratio, mean drop axis ratio, and magnitude of drop axis ratio variation) reflect the changes of drops orientation, drops shape as well as drops vibration.

To count the contribution of vibration component into the receiving signal, the simulation of drop vibration impact for the cases of different drop size distributions was presented in [21]. Computer simulation demonstrated and proved the fact that it is possible to fix the drop oscillation and shape deformation with the received signal by the selection of the polarization angle of the receiving antenna.

https://doi.org/10.1017/S1759078720000732 Published online by Cambridge University Press

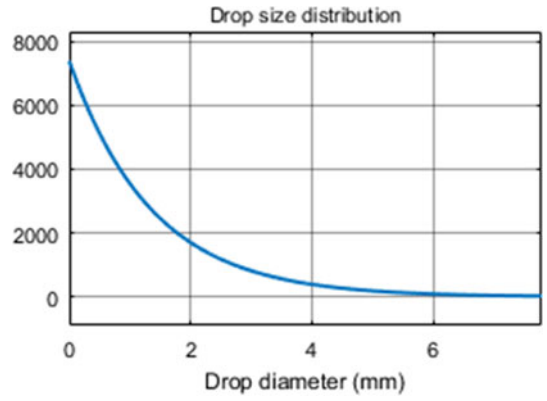


Fig. 4. Drop size distribution for $\mu = 0$.

The polarization angle of receiving antenna that allows excluding the contribution of drop deformation and vibration into the received signal is equal to 54.7°. The polarization angle of receiving antenna that allows extracting the contribution of drop deformation and vibration from the field reflected by a liquid hydrometeor is equal to 144.7°.

In [21, 22], it was shown and substantiated the possibility to detect wind-related phenomena with radar polarimetry. The methods come from the consideration that wind and wind-related phenomena affect the shape of the falling oblate drop-spheroid leading to the appearance of canting angle distribution [23,24].

In this paper, we consider the influence of wind of different speeds and the same direction onto the drops assemble and thus onto the reflections from liquid hydrometeors receive with a multi-polarization radar system.

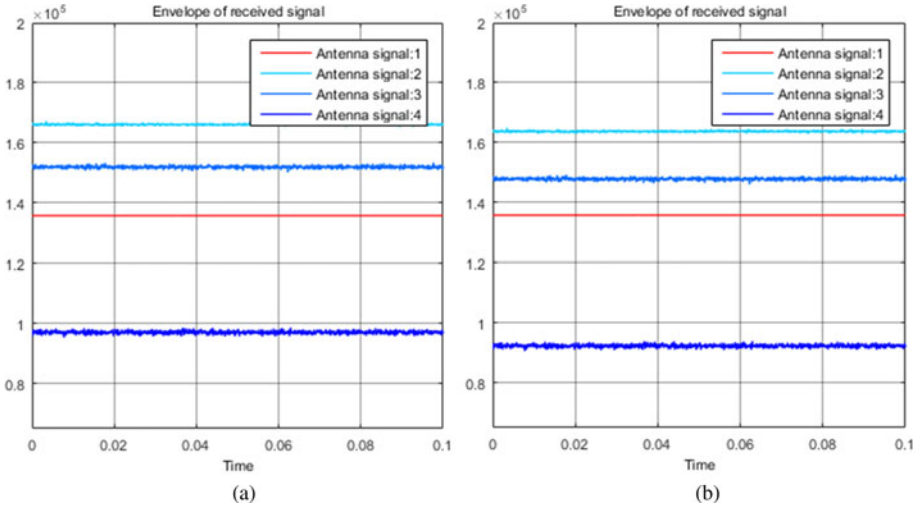


Fig. 5. (a) Magnitudes of electrical field components. Calm atmosphere for the case $\mu = 0$. (b) Magnitudes of electrical field components. Light wind for the case $\mu = 0$.

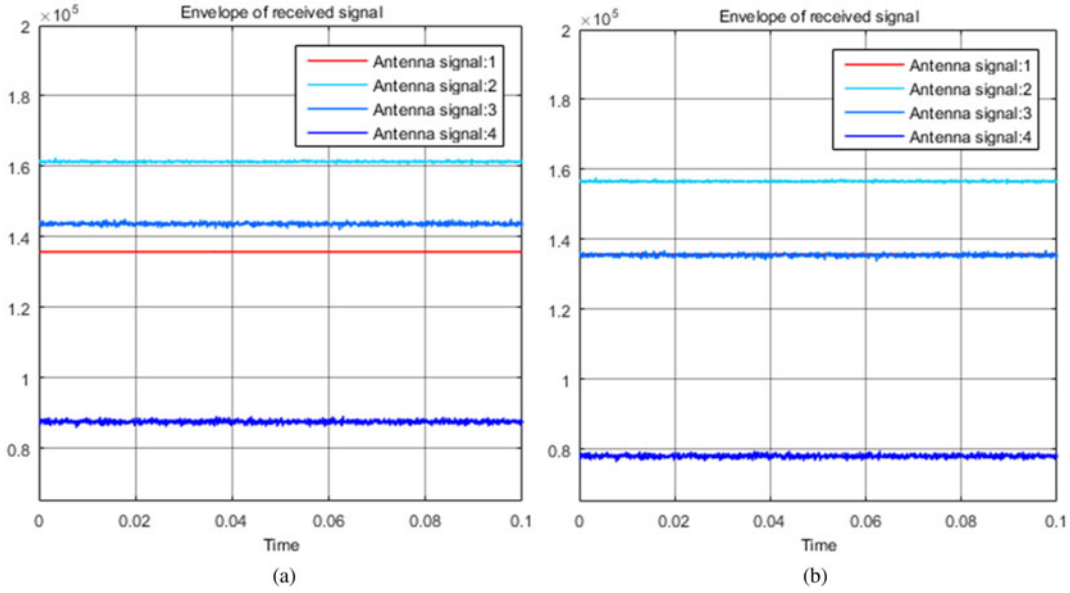


Fig. 6. (a) Magnitudes of electrical field components. Moderate wind for the case $\mu = 0$. (b) Magnitudes of electrical field components. Strong wind for the case $\mu = 0$.

https://doi.org/10.1017/S1759078720000732 Published online by Cambridge University Press

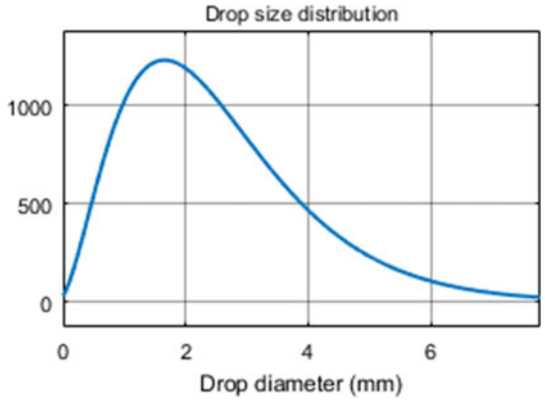


Fig. 7. Drop size distribution for $\mu = 2$.

Simulation results

The simulation was made in Simulink for the multi-polarization radar system depicted in [25]. The radar system includes four receiving antennas with polarization angles: 54.7, 84.7, 114.7, and 144.7°. The calculations were made for different cases of drop size distribution and different wind velocities. The simulations of electrical field component obtained by receivers with arbitrary polarization were made for the cases of calm atmosphere and wind of different speeds (weak, moderate, and strong).

The first simulations were performed for a widely used Marshall–Palmer distribution with $\mu = 0$ (Fig. 4). This case corresponds to the rather stable atmosphere that is characterized by the formation of stratus or stratocumulus clouds [19]. Stratus clouds, in turn, consist of minute particles mostly and give precipitation in the form of drizzle. Drop sizes vary normally from 0.2 to 0.5 mm in precipitation of this type.

The simulation results of electrical field component variation at four receiving antennas are shown in Figs 5 and 6. Antenna signal 1 corresponds to polarization 54.7°, antenna signal 2 corresponds to polarization 84.7°, antenna signal 3 corresponds to polarization 114.7°, and antenna signal 4 corresponds to polarization 144.7°.

The next simulation is performed for the Hrgian–Mazin distribution and $\mu = 2$ (Fig. 7). This case considers an increased number of larger drops that indirectly can be connected with both convection and wind that are required for drops coalescence and thus with drop growth. It is considered that Hrgian–Mazin distribution fits for clouds' microstructure simulation [26].

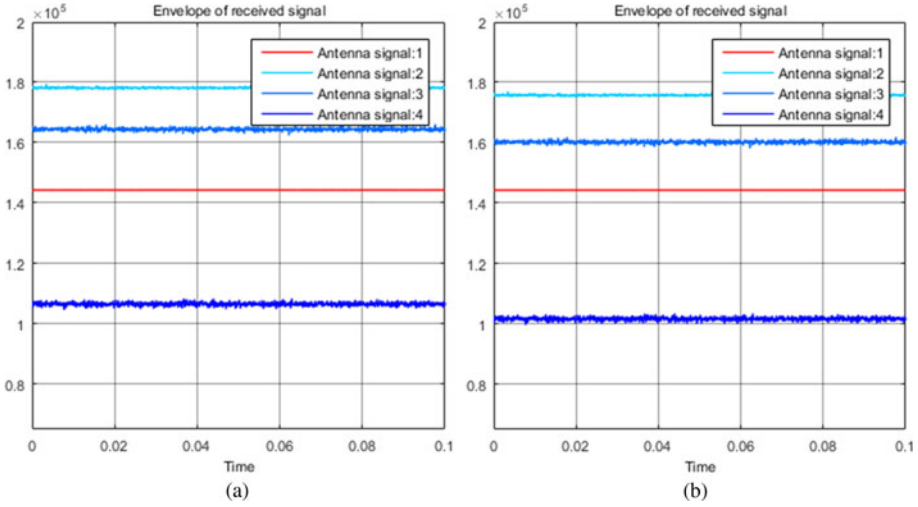


Fig. 8. (a) Magnitudes of electrical field components. Calm atmosphere for the case $\mu = 2$. (b) Magnitudes of electrical field components. Light wind for the case $\mu = 2$.

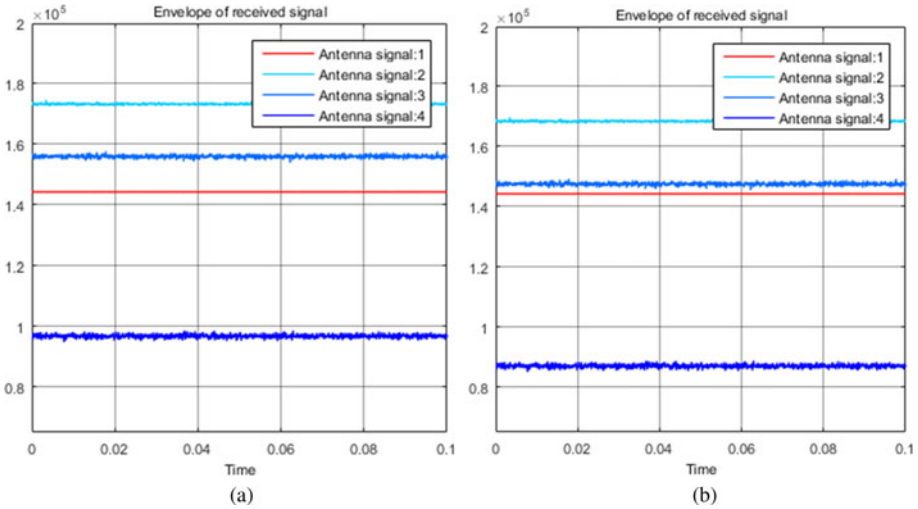


Fig. 9. (a) Magnitudes of electrical field components. Moderate wind for the case $\mu = 2$. (b) Magnitudes of electrical field components. Strong wind for the case $\mu = 2$.

https://doi.org/10.1017/S1759078720000732 Published online by Cambridge University Press

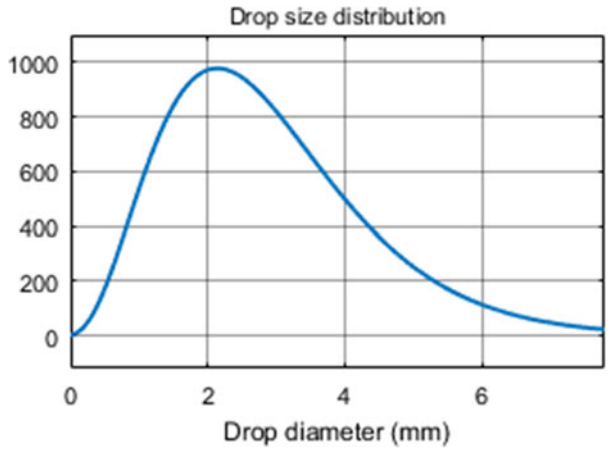


Fig. 10. Drop size distribution for $\mu = 3$.

The simulation results of electrical field component variation at four receiving antennas for drop size distribution with $\mu = 2$ are shown in Figs 8 and 9.

Drop size distribution with $\mu = 3$ (Fig. 10) has an increased number of drops with diameters from 2 to 2.5 mm. This simulation reflects precipitation with relatively larger drops that, in turn, corresponds more to significant clouds, stronger precipitation, and stronger wind-related phenomena.

The simulation results of electrical field component variation at four receiving antennas for drop size distribution with $\mu = 3$ are shown in Figs 11 and 12.

Energy levels received by the antennas of the multi-polarized radar system are different in all the figures and are affected by clouds and precipitation microstructure, polarization angle of the receiving antenna, and winds. Generally, the energy level increases with an increasing parameter μ of drop-size distribution. This corresponds to nature because the larger drop gives a stronger reflection of the radar signal. The maximum level of received energy is not found at the antenna with the polarization of the sounding waveform (54.7°). This is an expected situation and can be explained by the difference in mutual orientation of antenna polarization basis and drop polarization basis. The minimum energy level is found at the antenna with a polarization of 144.7° for all cases of the drop size distributions and wind force. This is the level of the "vibrating" component of energy reflected from drops assemble that allows fixating the drop oscillation or drop vibration magnitude. This proves the fact

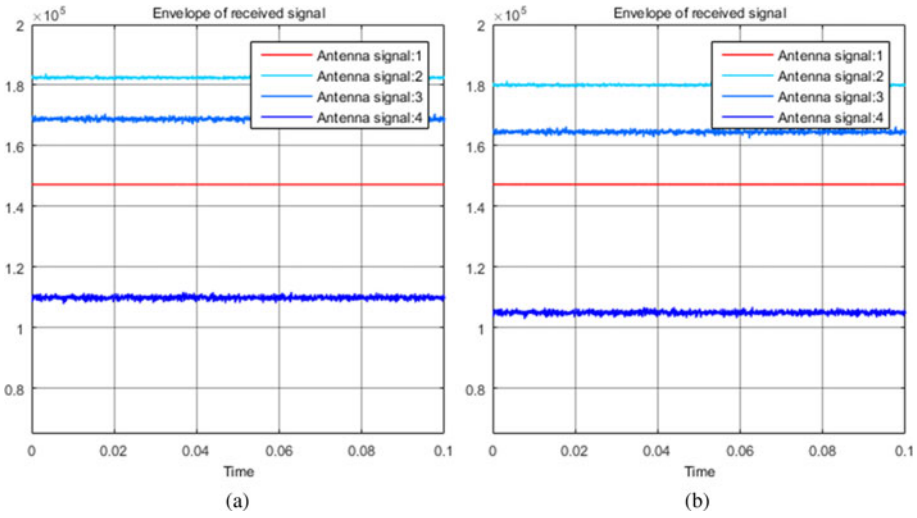


Fig. 11. (a) Magnitudes of electrical field components. Calm atmosphere. (b) Magnitudes of electrical field components. Light wind.

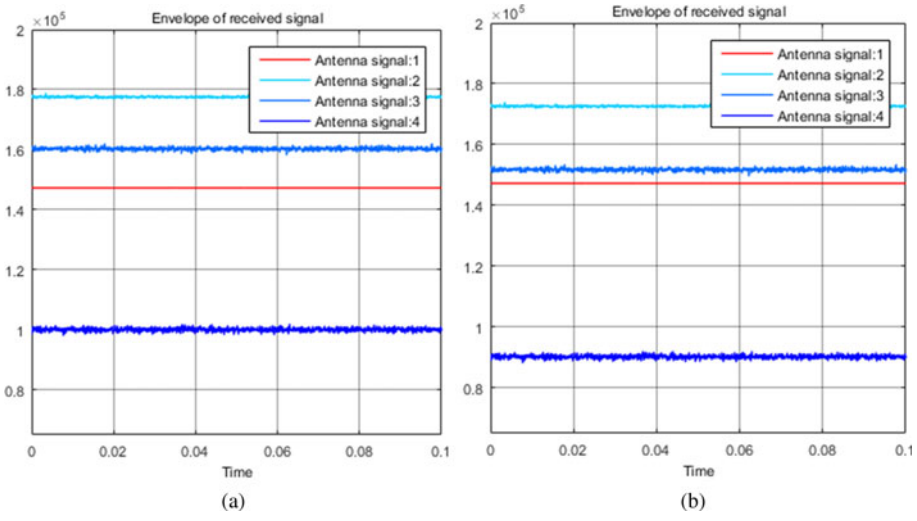


Fig. 12. (a) Magnitudes of electrical field components. Moderate wind. (b) Magnitudes of electrical field components. Strong wind.

https://doi.org/10.1017/S1759078720000732 Published online by Cambridge University Press

that changing the polarization of receiving antennas allows separating the constant component of reflected from hydrometeor assemble signal and vibrating one.

When wind affects the drops assemble, the energy level decreases at all antennas of multi-polarization radar. This is true for all cases of drop size distributions shown in Figs 5, 6, 8, 9, 11 and 12. This fact can be explained as the influence of the change of drop axis ratio under the wind effect.

At the same time, it is noticeable that the energy levels received by different antennas are changed in different ways. The most significant energy drop with wind force growth is observed for the antenna that is adjusted to receive signals with the polarization of 114.7°. This antenna has 60° polarization differences with the polarization of the sounding waveform. It is remarkable that the difference in signal levels received at the antennas 54.7 and 114.7° decreases with the increase of wind for all drop-size distributions. However, this difference increases when μ of the wind increases. Taking into account the nature of clouds and precipitation formation, one can say that the increase of parameter μ is indirectly connected to the appearance and strengthening of wind-related phenomena. This is because wind, turbulence, downdraughts, and updraughts contribute to drop growth by means of coalescence or capture effect. Signal levels received at antenna 114.7° with respect to the antenna tuned to receive signal with the polarization of 54.7° decrease due to wind effect much more significant than the total signal level growth as wind increases when the parameter μ is larger.

Therefore, it can be suggested that information about mutual signal level redistribution can indicate the microstructure of clouds and precipitation as well as the force or intensity of wind-related phenomena. It can be realized in the modern meteorological radar, particularly of C and S bands.

Conclusion

In this paper, the mathematical expression for calculating the magnitude of electrical field components obtained by receiving antennas with arbitrary polarization is realized. The expression takes into account the appearance of drop canting and drops axis ratio variation caused by the wind.

Simulation of the energy redistribution of the signal reflected from liquid hydrometeors assemble over the antennas of multi-polarimetric radar for the cases of stable atmosphere and for the cases of light, moderate and strong wind is done and analyzed for different drop size distributions.

The simulation results demonstrate the possibility to register wind and wind-related phenomena by polarimetric radar additionally to traditional tasks of radar polarimetry.

The results of the paper can be used to exclude the impact of drop vibration and oscillation into the radar signal to eliminate errors and underestimation during parameter measurements. These can be used as well for segregation of reflected signal magnitude variation due to the wind-related phenomena from other factors.

References

1. **Lhermitte RM** (1973) Meteorological Doppler radar. Science. 1982: N 4109, pp. 258–262.
2. **Doviak RJ and Zrnic DS** (1993) *Doppler Radar and Weather Observations*. San Diego: Academic Press, Inc.
3. **Ryzhkov AV and Zrnic DS** (2019) *Radar Polarimetry for Weather Observations*. Cham: Springer.
4. **Rayleigh JWS** (1879) On the capillary phenomena of jets. *Proceedings of the Royal Society of London* **19**, 71–97.
5. **Pruppacher HR and Beard KV** (1970) A wind tunnel investigation of the internal circulation and shape of water drops falling at terminal velocity in air. *Quarterly Journal of the Royal Meteorological Society* **96**, 247–256.
6. **Pruppacher HR and Pitter RL** (1971) A semi-empirical determination of the shape of cloud and rain drops. *Journal of Atmospheric Sciences* **28**, 86–94.
7. **Beard KH and Chuang C** (1987) A new model for equilibrium shape of rain drops. *Journal of Atmospheric Sciences* **28**, 1509–1524.
8. **Tokay A and Beard KV** (1996) A field study of raindrop oscillations. Part I: observation of size spectra and evaluation of oscillation causes. *Journal of Applied Meteorology* **35**, 1671–1687.
9. **Szakall M, Diehl K and Mitra SK** (2009) A wind tunnel study on the shape, oscillation and internal circulation of large raindrops with sized between 2.5 and 7.5 mm. *Journal of Atmospheric Research* **66**, 755–765.
10. **Szakall M, Mitra SK, Diehl K and Borrmann S** (2010) Shapes and oscillations of falling raindrops. *Journal of Atmospheric Research* **97**, 416–425.
11. **Kubesh RJ and Beard KV** (1993) Laboratory measurements of spontaneous oscillations for moderate-size raindrops. *Journal of Atmospheric Sciences* **50**, 1089–1098.
12. **Goddard JWF and Cherry SM and Bringi VN** (1982) Comparison of Dual-Polarization Radar Measurements of Rain with Ground-Based Disdrometer Measurement. *Journal of Applied Meteorology* **21**, 252–256.
13. **Averyanova Y, Yanovsky F and Averyanov A** (2011) Connection of reflected radar signal with liquid-hydrometeor deformation rate. *Proceedings of the 3rd Symposium on Microwaves, Radar and Remote Sensing*, Kiev, Ukraine, August 25–27, 2011, pp. 217–219.
14. **Averyanova YA, Rudiakova AN and Yanovsky FJ** (2017) Multi-polarization approach to operative dangerous atmospheric phenomena detection. *Proceedings of the 5th Symposium on Microwaves, Radar and Remote Sensing*, Kiev, Ukraine, August 29–31, 2017, pp. 245–248.
15. **Averyanova YA, Braun I, Rudiakova AN and Yanovsky FJ** (2018) Reflected signal variations simulation and estimation when multi polarization measurements. *Proceedings of 22nd Microwave and Radar Conference (MIKON 2018)*, May 15–17, 2018, Poznan, Poland, pp. 1–4.
16. **Averyanova YA, Rudiakova AN and Yanovsky FJ** (2017) Segregating deformation of scattering rain-drops using several receive antennas with different polarization angles. *Proceedings of International Radar Symposium (IRS 2017)*, June 28–30, 2017, Prague, Czech Republic. pp. 1–4.
17. **Averyanova YA, Rudiakova AN and Yanovsky FJ** (2017) Multi-polarization approach to liquid hydrometeors' vibration discrimination in presence of turbulence. *Proceedings of Signal Processing Symposium SPS-2017*, 12–14 September 2017, Debe near Warsaw, Poland. pp. 1–4.
18. **Gorelik AG** (1989) Influence of raindrops vibration on polarization characteristics of radar echo. *Physics of Atmosphere and Ocean* **25**, 960–968 (in Russian).
19. **Marshall JS and Mc K. Palmer W** (1948) The distribution of raindrops with size. *Journal of Meteorology* **5**, 165–166.
20. **Fog NI** (2004) The representation of rainfall distribution and kinetic energy. *Hydrology and Earth System Sciences* **8**, 1001–1007.
21. **Averyanova YA, Rudiakova AN and Yanovsky FJ** (2018) Drop oscillation estimate with multi-polarization radar. *Proc. of 17th International Conference on Mathematical Methods in Electromagnetic Theory*, Kyiv, Ukraine. pp. 342–345.
22. **Averyanova YA, Averyanov A and Yanovsky FJ** (2007) Analysis of the possibility to determine wind parameters ahead the aircraft by using polarimetric airborne radar. *Telecommunications and Radioengineering* **66**, 1103–1112.
23. **Averyanova YA, Averyanov AA and Yanovsky FJ** (2002) Wind condition model of flight. *Proceedings of International Conference on Mathematical Methods in Electromagnetic Theory*, Kiev 2002, Ukraine, vol. **1**, pp. 275–277.
24. **Russchenberg HWJ** (1992) *Ground-based Remote Sensing of Precipitation Using a Multi-Polarized FM-CW Doppler Radar*. Delft: Delft University Press.
25. **Averyanova YA, Rudiakova AN, Braun I and Yanovsky FJ** (2018) Simulations of multi polarization measurements and reflected signal magnitude variations caused by turbulence. *Proceedings of International Radar Symposium (IRS 2018)*, June 19–22, 2018, Bonn, Germany, pp. 1–5.
26. **Mazin IP** (1989) Microstructure of Clouds. In Mazin IP and Hrgian AH (eds), *Clouds and Cloudy Atmosphere*. Leningrad: Gidrometeoizdat, pp. 297–344.

https://doi.org/10.1017/S1759078720000732 Published online by Cambridge University Press



Yuliya Averyanova received her Ph.D. in Engineering in 2005 and Doctor of Science in Navigation and Traffic Control in 2017 from the National Aviation University of Ukraine. Currently, she is Professor of Air Navigation Systems Department at NAU. Her main research interests are radar, remote sensing, signal processing, radar polarimetry, meteorology, Doppler, and polarimetric radar.



Anna Rudiakova received combined B.Sc. and M.Sc. degrees in Radio Physics and Electronics from Donetsk State University in 1997 and received her Ph.D. in Computer Systems and Components from the National Technical University of Ukraine at "Kyiv Polytechnic Institute" in 2009. She became an associate university professor in 2011. Her main research interests are signal processing in radiolocation and remote sensing, optoelectronic signal-processing devices, and embedded electronic systems.



Felix Yanovsky received his Ph.D. from the Moscow State Technical University (MSTUCA), USSR in 1979, and two D.Sc. from the National Aviation University (NAU) in Kyiv, Ukraine (1992) and MSTUCA (1993). Currently, he is Full Professor and the Head of Electronics, Robotics, Monitoring and IoT Technologies Department at NAU, and IEEE Ukraine Section Chair. He has published more than 550 papers, books, and invention patents. He is an IEEE Fellow, EuMA member, and State Prize Winner of Ukraine in the field of Science and Technology. Currently, his main research interests are in radar, remote sensing, Doppler polarimetry, signal processing, and multi-parametric and adaptive measurements.

https://doi.org/10.1017/S1759078720000732 Published online by Cambridge University Press